Novel large-area, low-pressure MSGCs for thermal neutron imaging using ^{157}Gd/CsI - converters

Speaker: B. Gebauer (HMI)

Collaborators: N. Chkhalo, Ch. Schulz, Th. Wilpert (HMI), S.F. Biagi (Liverpool), ...

Outline:

1. Gaseous vs. solid state converters:
   Position resolution, detection efficiency
2. HMI detector design
3. 2D-MSGC multilayer manufacturing technology
4. MSGC low-pressure, 2-stage amplification:
   Simulation results (MAXWELL, MSGCSIM)
5. Measured MSGC and MDOT data
6. Delay line readout optimization (SPICE)
7. Data acquisition
8. Summary and outlook: solved and open problems

Thermal neutron (1.8 Å) capture reactions

Converter type	Reaction	n_{th} Absorption length λ_n n_{th} Capture cross section	Ejectile range R/ atten. length λ_{ce} Ejectile energies [keV]
Gas	$^{3}He\ (n,p)t$	$\lambda_n = 7.59$ bar cm 5 333 b	$R_p = 0.43$ bar cm CF_4 p: 573, t: 191
	$^{6}Li\ (n,\alpha)t$	$\lambda_n = 230\,\mu m$ 940 b	$R_t = 130\,\mu m$ t: 2 727, α : 2 055
	$^{10}B\ (n,\alpha)^{7}Li$	$\lambda_n = 19.9\,\mu m$ 3 836 b	$R_\alpha = 3.14\,\mu m$ α : 1 472, ^{7}Li: 840 (93.6%)
Foil	$^{157}Gd\ (n,\gamma)^{158}Gd^*$ Abund. 15.65%, $E^* = 7\,937$	$\lambda_n = 1.30\,\mu m$ 255 000 b	$\lambda_{ce} = 11.6 \pm 0.3\,\mu m$ ce: 29 - 182 (87.3 ± 2.5%)
	$^{155}Gd\ (n,\gamma)^{156}Gd^*$ Abund. 14.80%, $E^* = 8\,536$	$\lambda_n = 5.38\,\mu m$ 61 400 b	ce: 39 - 191 (84.5 ± 5%)
	$^{nat}Gd\ (n,\gamma)$	$\lambda_n = 6.72\,\mu m$ 49 122 b	$\lambda_{ce} = 12.3 \pm 0.3\,\mu m$ ce: 29 - 191 (86.5 ± 1%)

^{157}Gd: R.C. Greenwood et al., Nucl. Phys. A 304 (1978) 327 - 428

^{155}Gd: A. Bäcklin et al., Nucl. Phys. A 380 (1982) 189 - 260

^{nat}Gd: C.K. Hargrove et al., Nucl. Instr. and Meth. A 357 (1995) 157 - 169

HMI SANS Detector - 1.5 bar ^3He + 0.25 bar CF_4

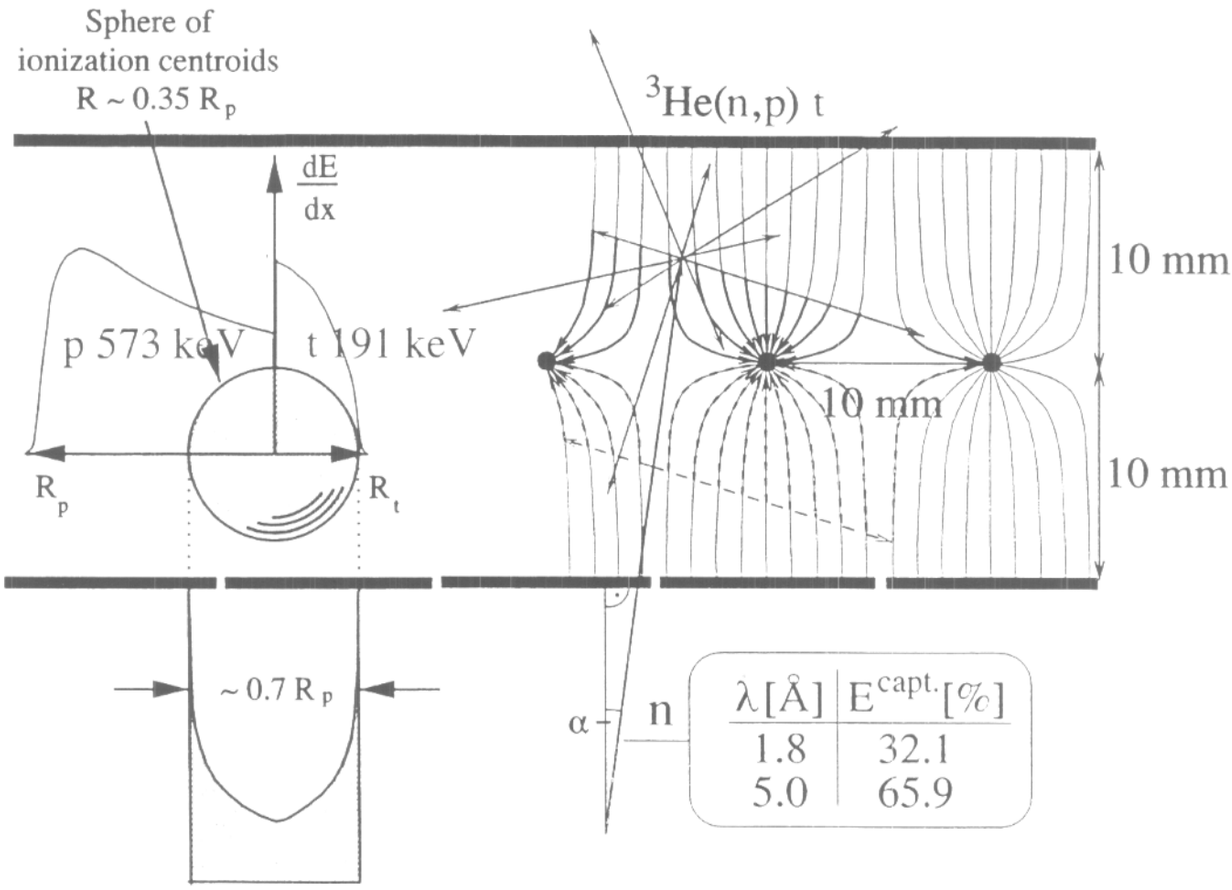

λ[Å]	$E^{capt.}$[%]
1.8	32.1
5.0	65.9

Energy loss vs. range for p (573 keV)

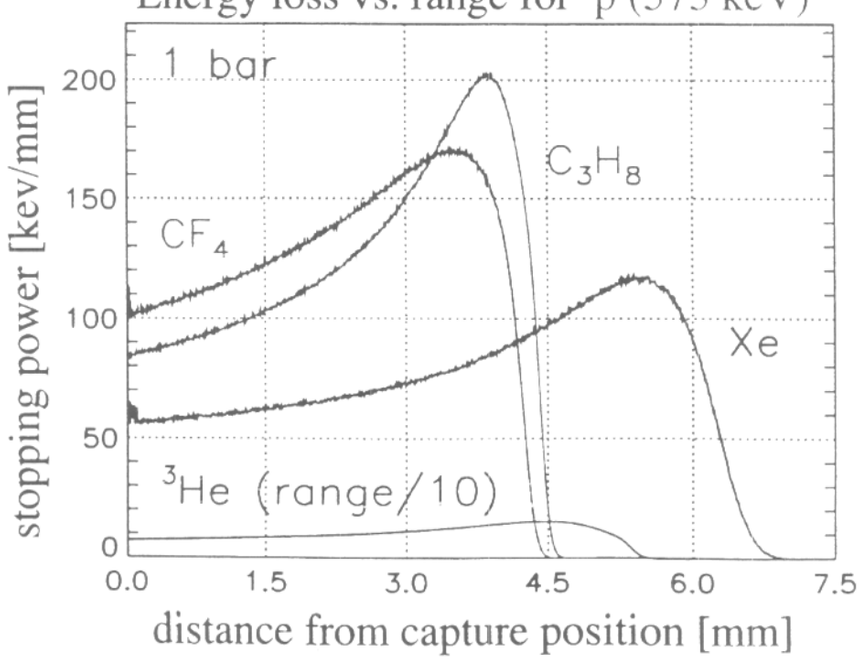

$^{157}_{64}Gd\,(n,\gamma)\,^{158}_{64}Gd$

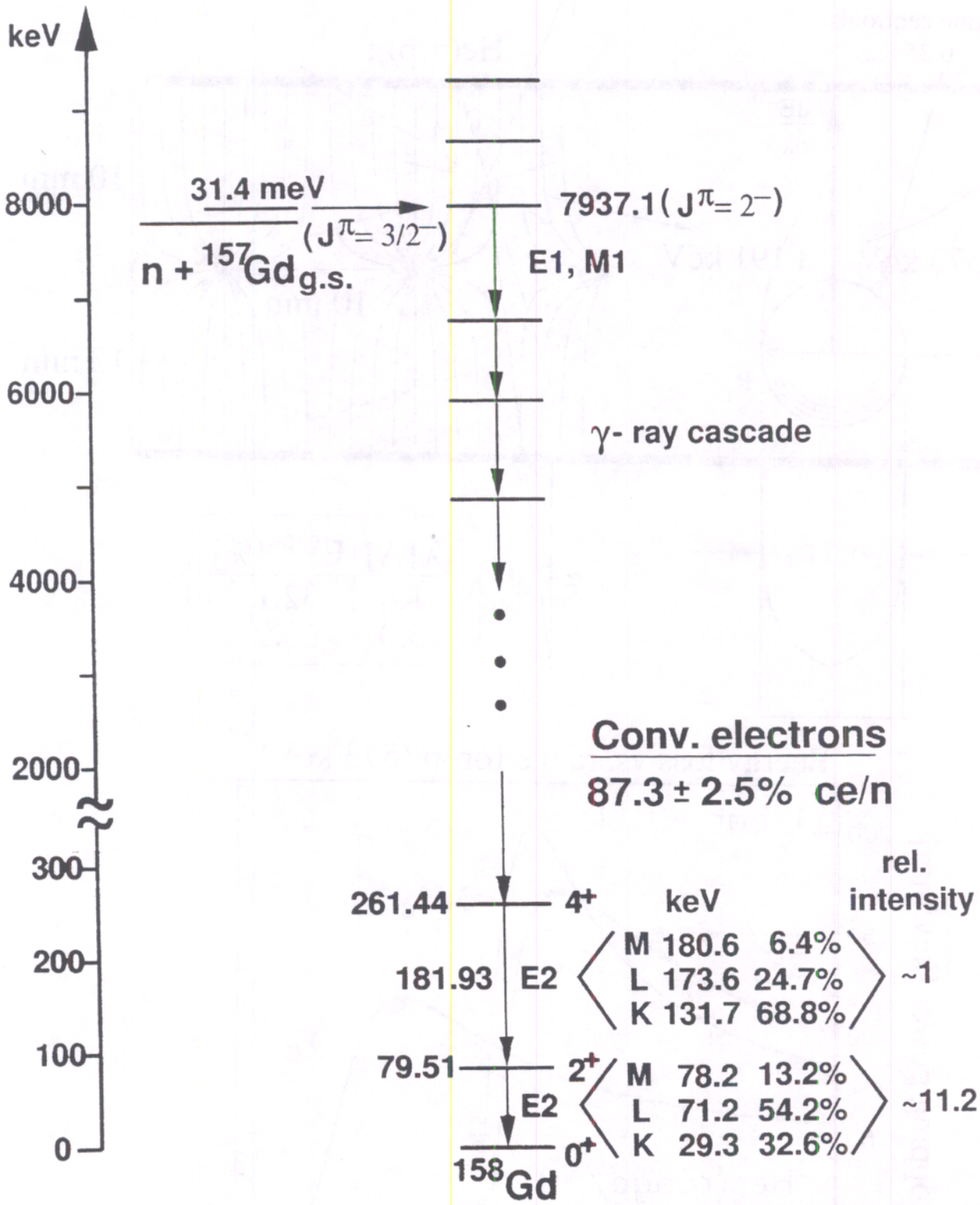

R.C. Greenwood et al.,
Nucl. Phys. A304 (1978) 327.

^{157}Gd/CsI n/e$^-$ converter efficiency

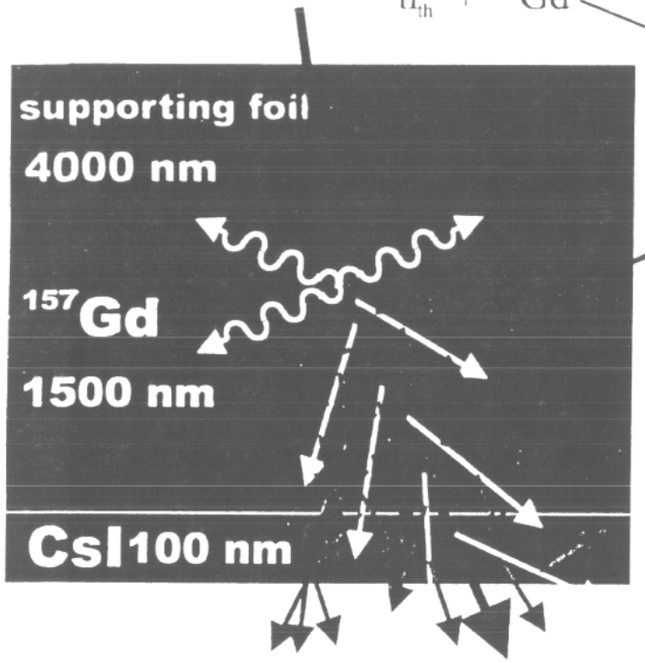

n_{th} + ^{157}Gd → γ–ray's → background

→ 87.3% conv. electrons (29 - 182 keV)

↓

δ–electrons (I_{max} = 50 eV)
escape length: 200-300 nm

↓

slow e$^-$ (eV) → solid CsI: 3-10 e$^-$
escape length: 30 nm

↓

porous CsI → with high extraction field
(controlled Malter effect)
10 e$^-$ - > 100 e$^-$

M.P. Lorikyan,
Physics-Uspekhi 38 (1995) 1271.

Isobutane 20 hPa

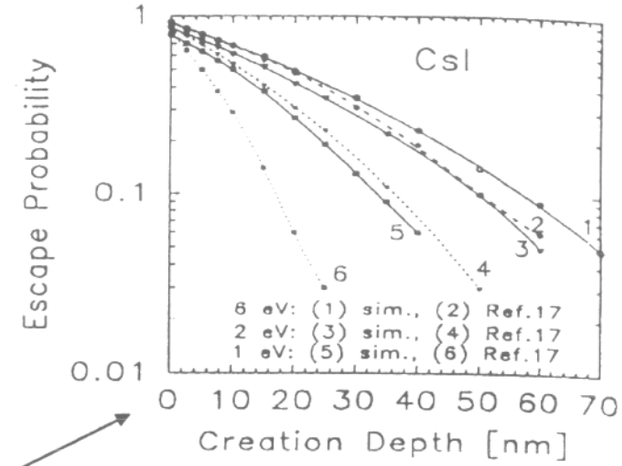

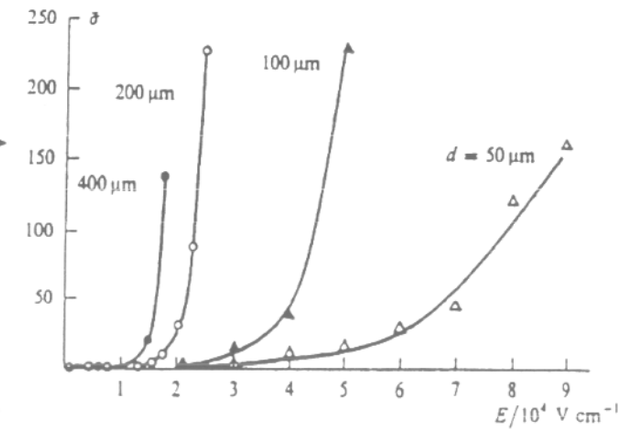

Average SEE coefficient $\bar{\sigma}$ for KCL (2%)

^{157}Gd
Conversion electron escape efficiency

$$E(d) = E_0 * e^{-\frac{d}{\lambda_{ce}}} * \{1 - e^{-\frac{d}{\lambda_n}}\}$$

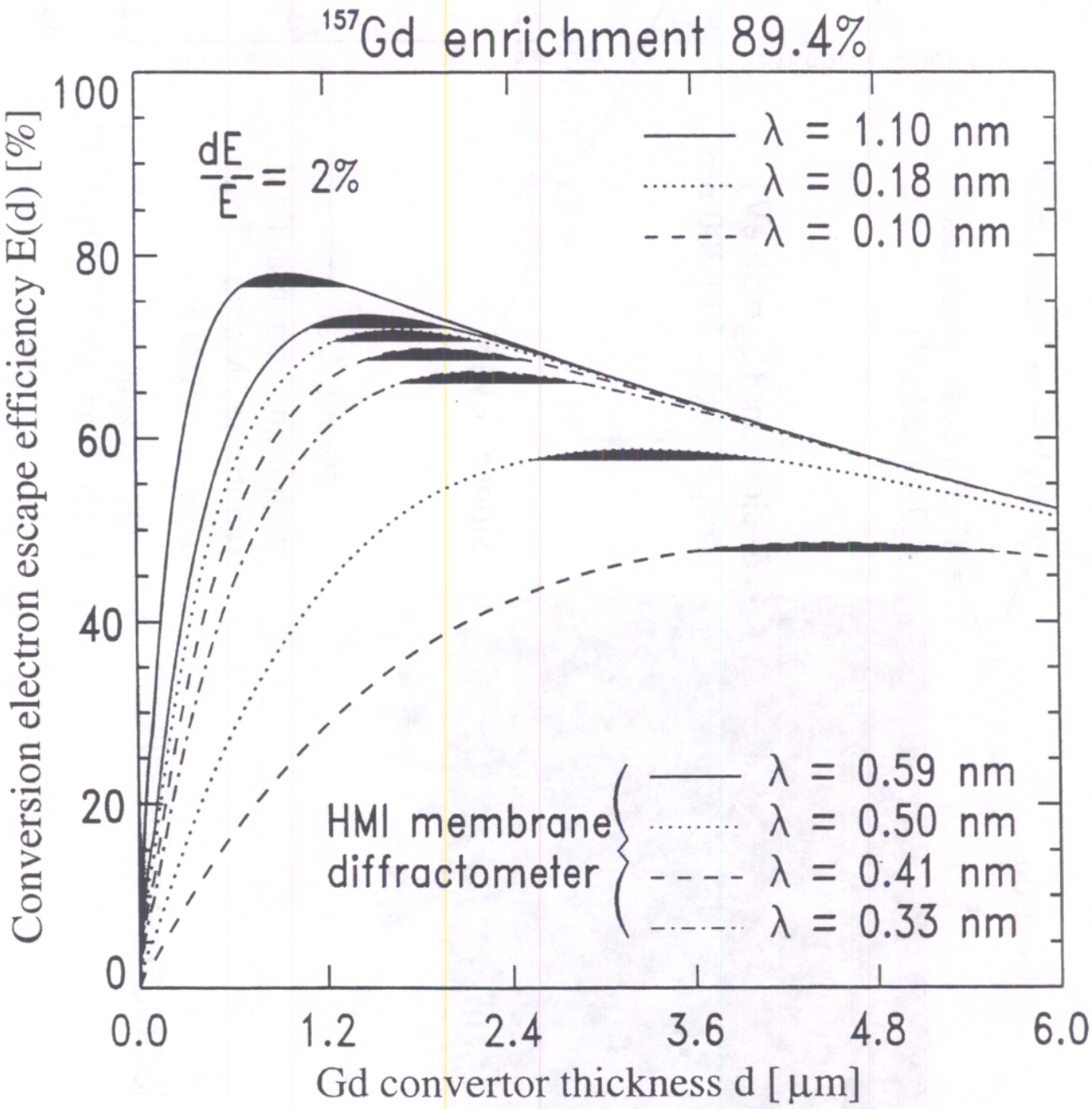

HMI 2D - MSGC detector schematic

B. Gebauer, Ch. Schulz, Th. Wilpert

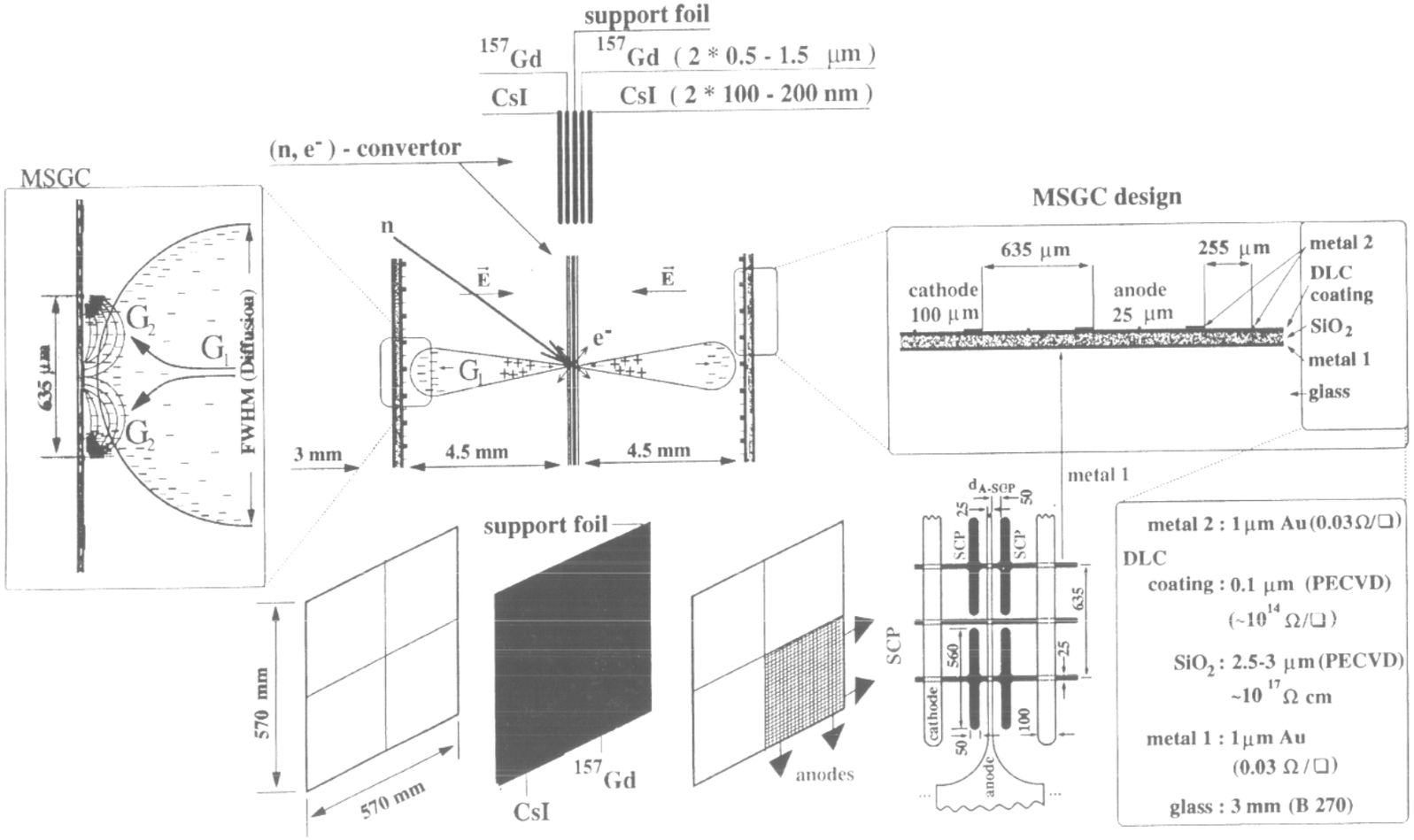

MSGC design

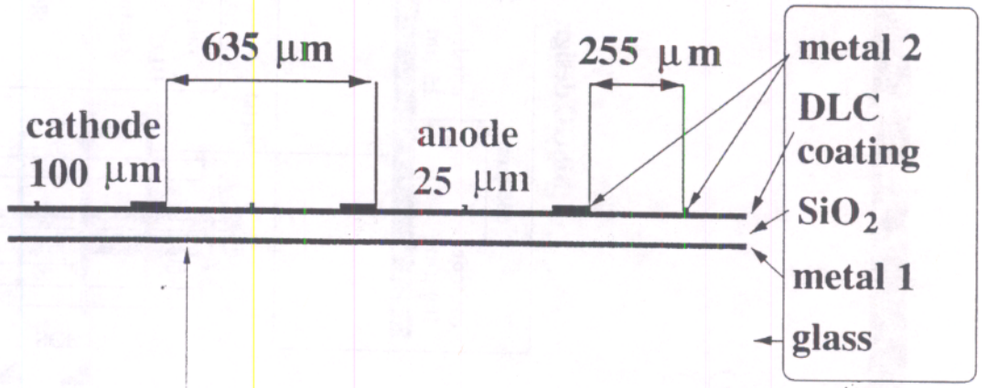

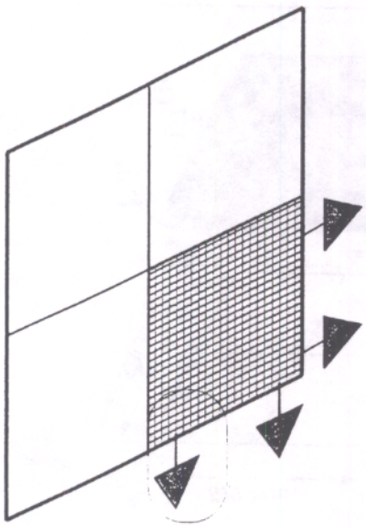

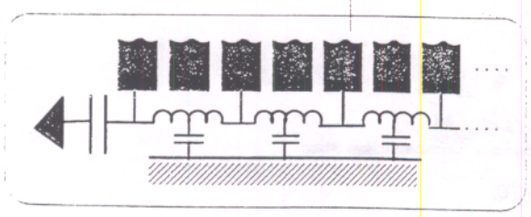

metal 2 : 1 μm Au (0.03 Ω/❑)

DLC

coating : 0.1 μm (PECVD)

($\sim 10^{13\text{-}14}$ Ω/❑)

SiO_2 : 2.5-3 μm (PECVD)

$\sim 10^{17}$ Ω cm

metal 1 : 1 μm Au

(0.03 Ω / ❑)

glass : 3 mm (B 270)

Field shaping in the gas volume with resistive DLC layer

equipotential lines without DLC

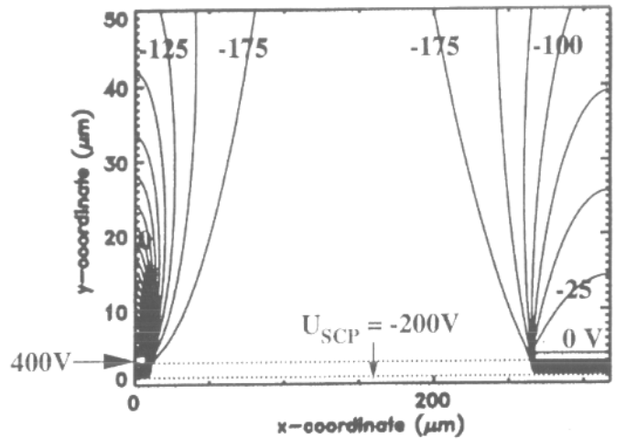

equipotential lines with DLC

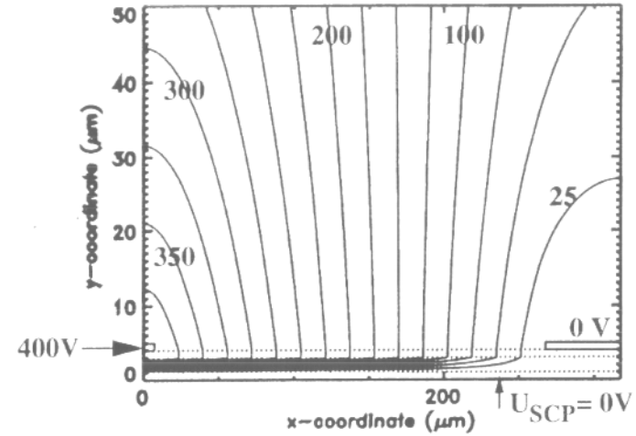

field strength variation with DLC

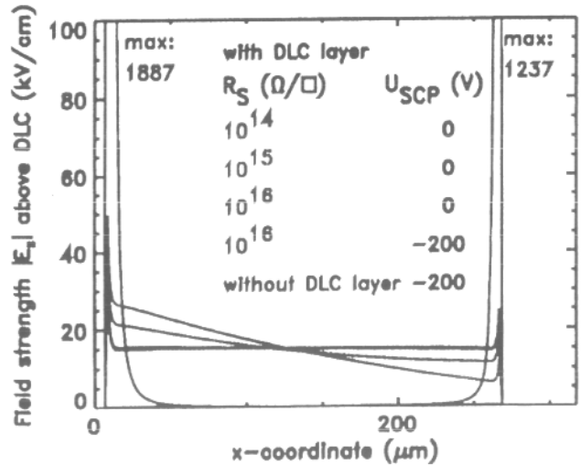

equipotential lines with DLC

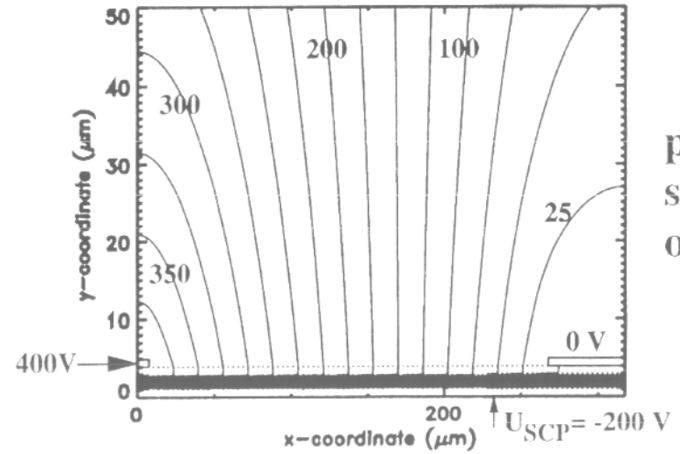

perfect screening of U_{SCP}

N-doped amorphous silicon carbide (a-SiCN:H) resistive layer

A. Weber et al., Frauenhofer-Institut für Schicht- und Oberflächentechnik, D-38108 Braunschweig

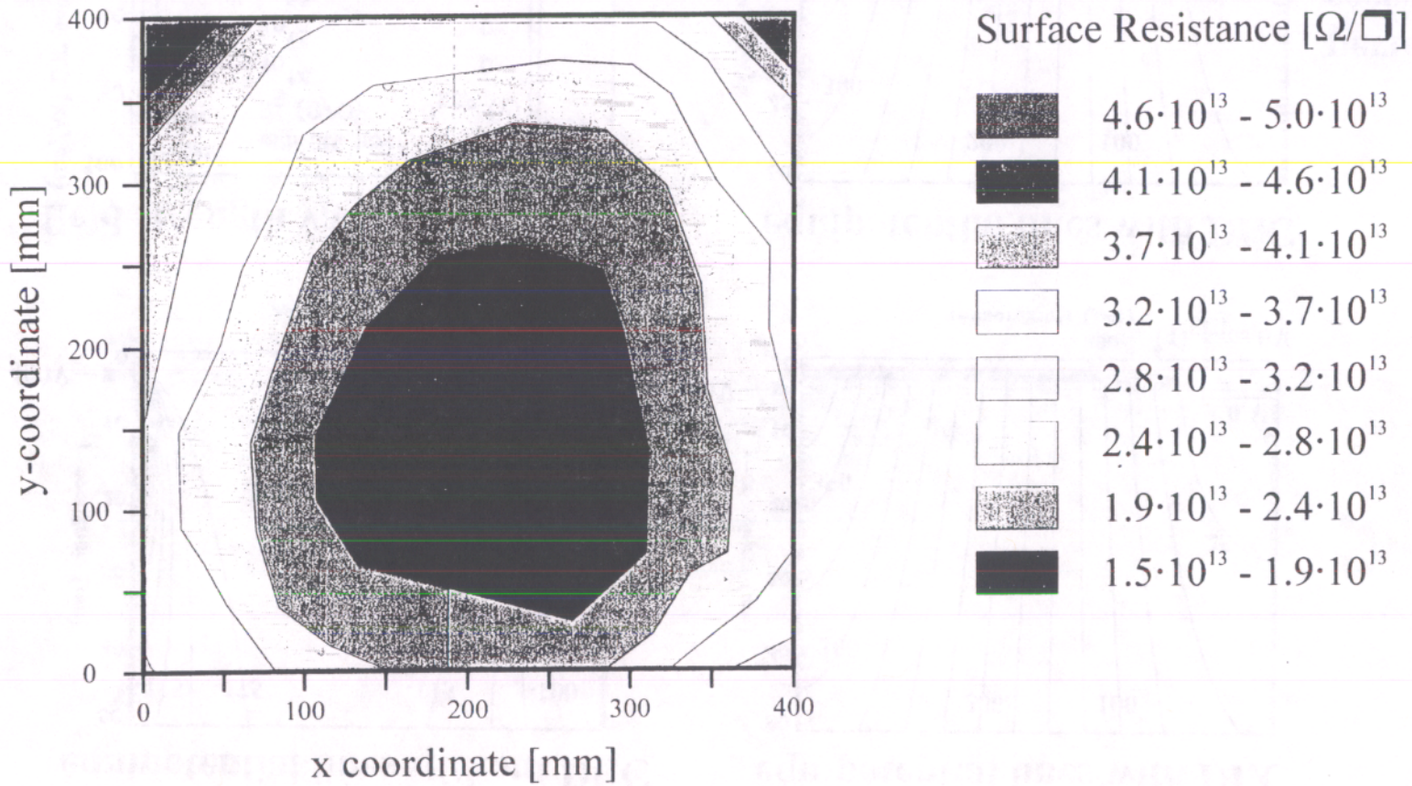

Low-pressure 2-stage avalanche multiplication (MSGC)

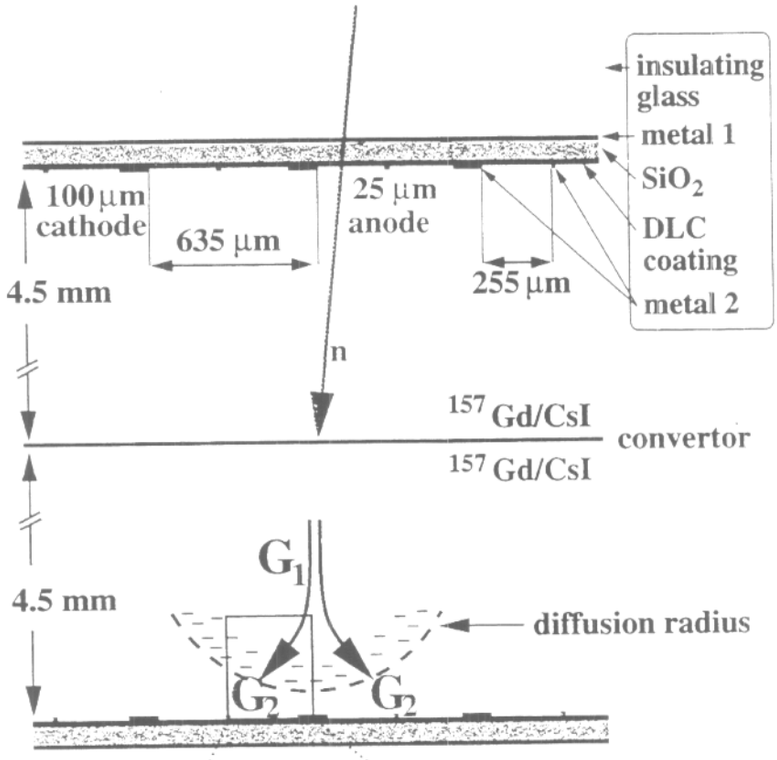

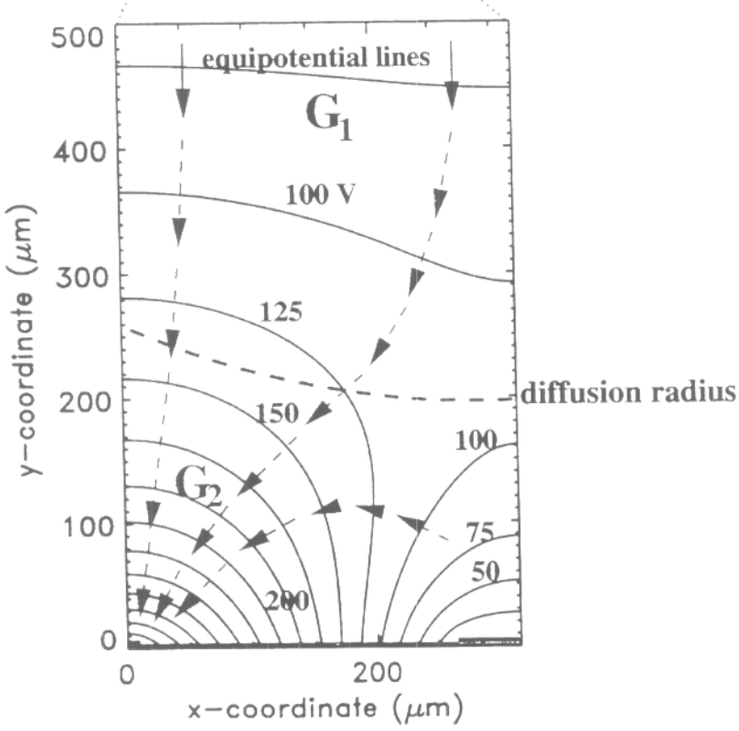

Low-pressure 2-stage avalanche multiplication

Ionisation Cross Section in Isobutane

St. F. Biagi, Nucl. Instr. and Meth. A310 (1991) 133

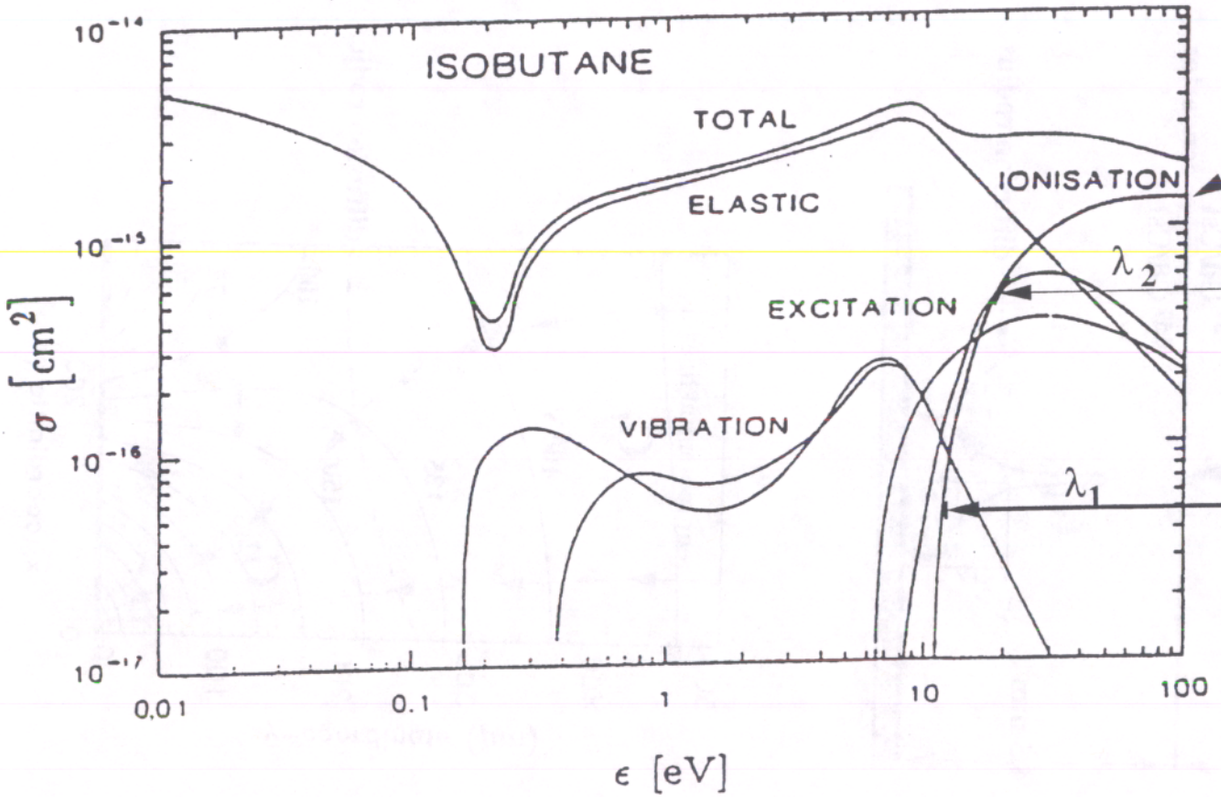

p = 20 mbar

λ_i^{max} = 16 μm

λ [μm]	ε [eV]
35 - 48	20 - 22
390 - 450	11.4 - 12.0

Low-pressure 2-stage avalanche multiplication (MSGC)

(Simulation results)

Gains G_1 (parallel plate), G_2 (microstrip) and $G = G_1 \times G_2$

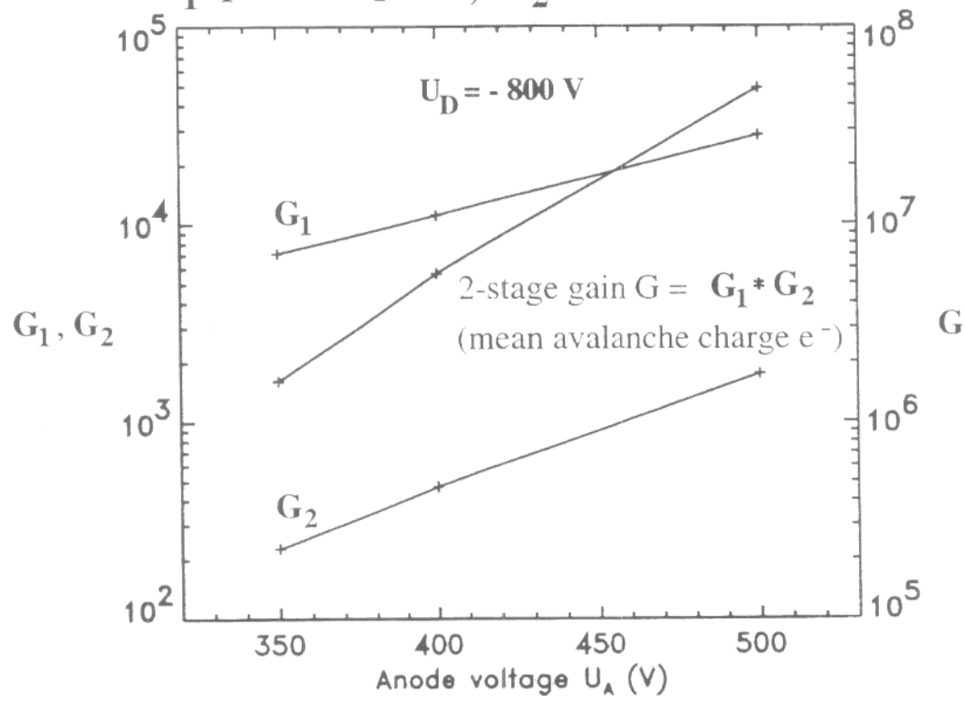

Electron number distribution q with Polya fit P(q)

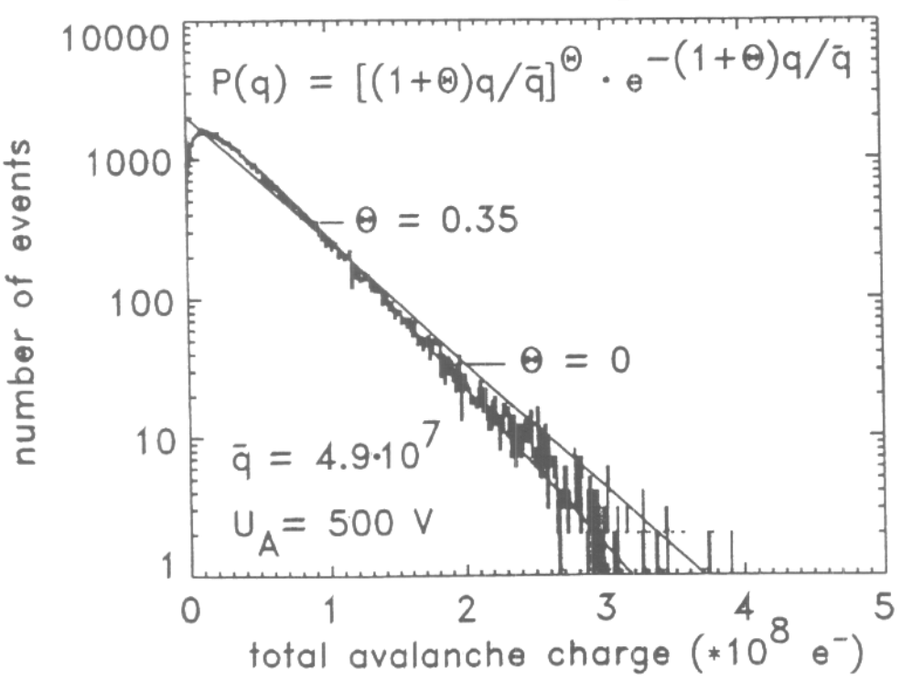

Low-pressure 2-stage avalange multiplication (MSGC)

(Simulation results)

Anode and SCP signals for $U_A = 400$ V and $d_{A\text{-}SCP} = 50\ \mu m$

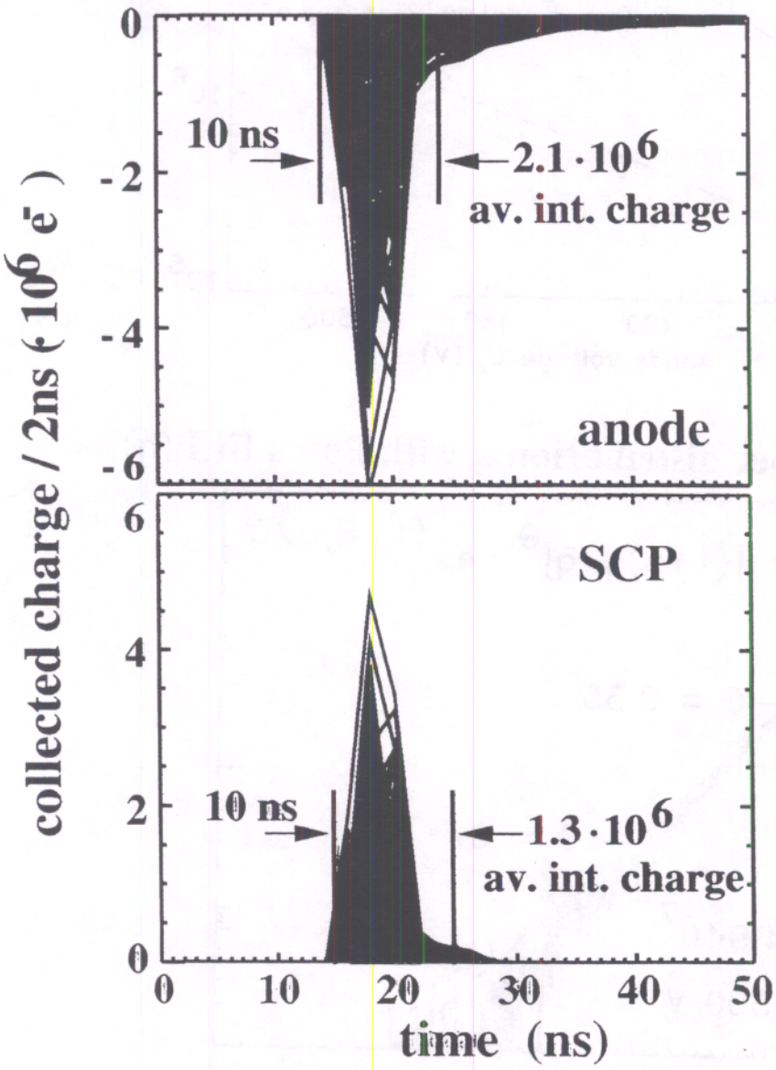

Low-pressure 2-stage avalanche multiplication (MSGC)
(Simulation results)

Detail of the microstrip and SCP layout

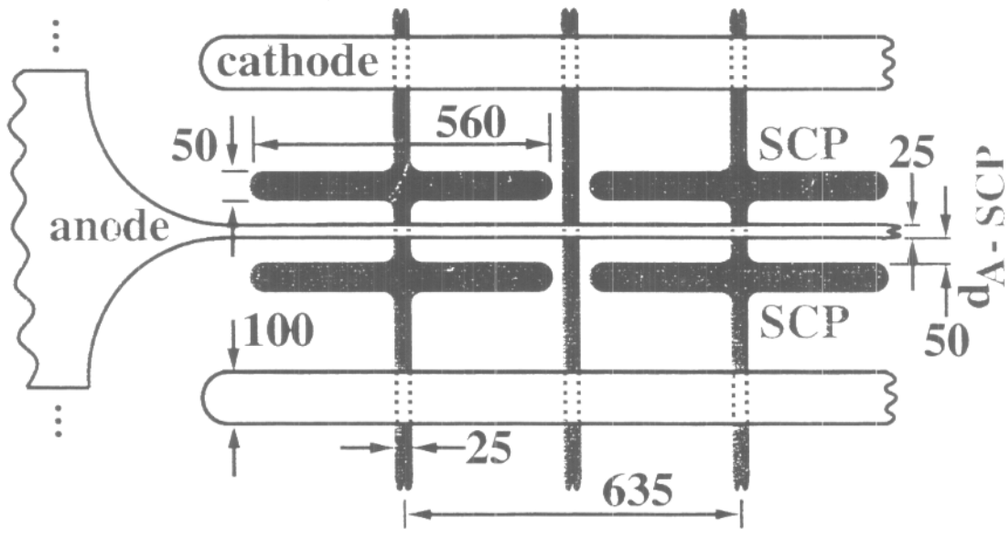

Induced signal charge vs. d_{A-SCP}

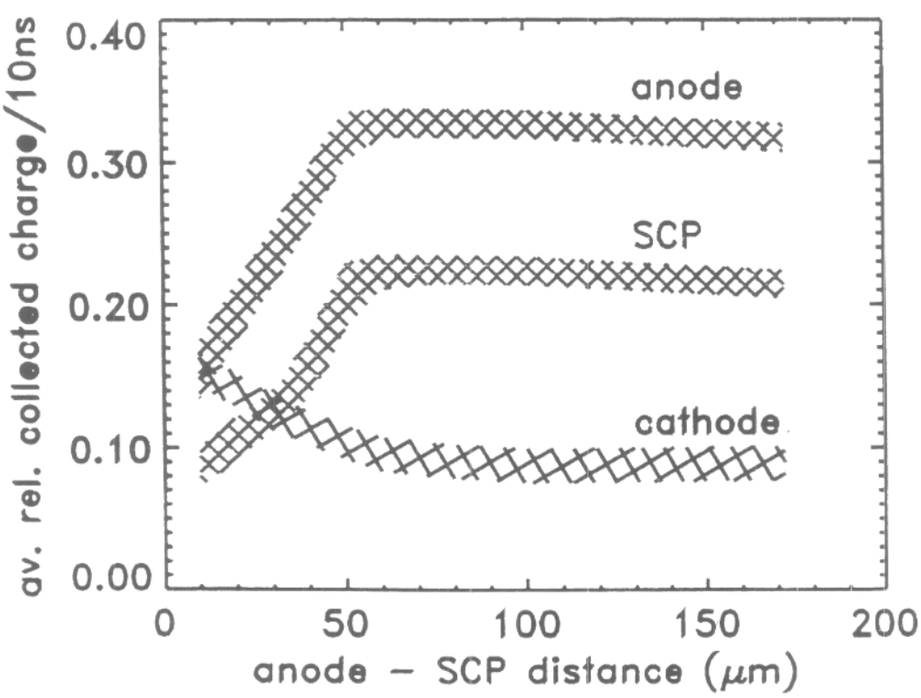

On the high gain operation of low-pressure microdot gas avalanche chambers

A. Breskin, R. Chechik, G. Garty, A. Pansky and E. Shefer
Department of Particle Physics
The Weizmann Institute of Science
Rehovot, 76100, Israel.

and

S.F. Biagi
Department of Physics
University of Liverpool
Liverpool L69 3BX
England, U.K.

a) The Microdot photon detector

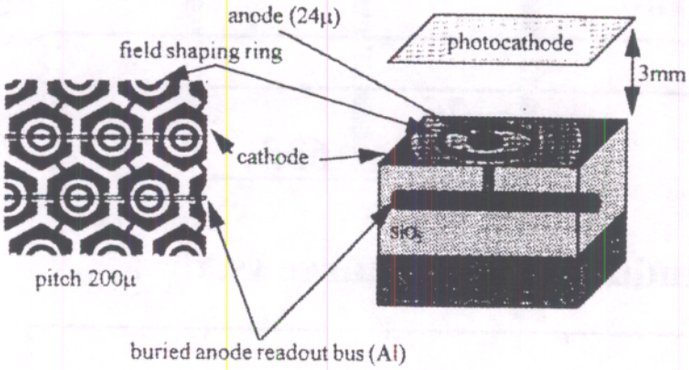

b)

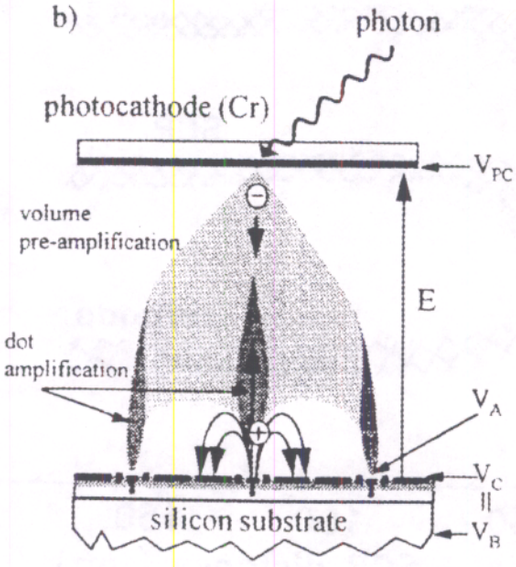

Measured MDOT single photon pulse-height spectra

30 torr C_3H_8 , 200 μm pitch structure

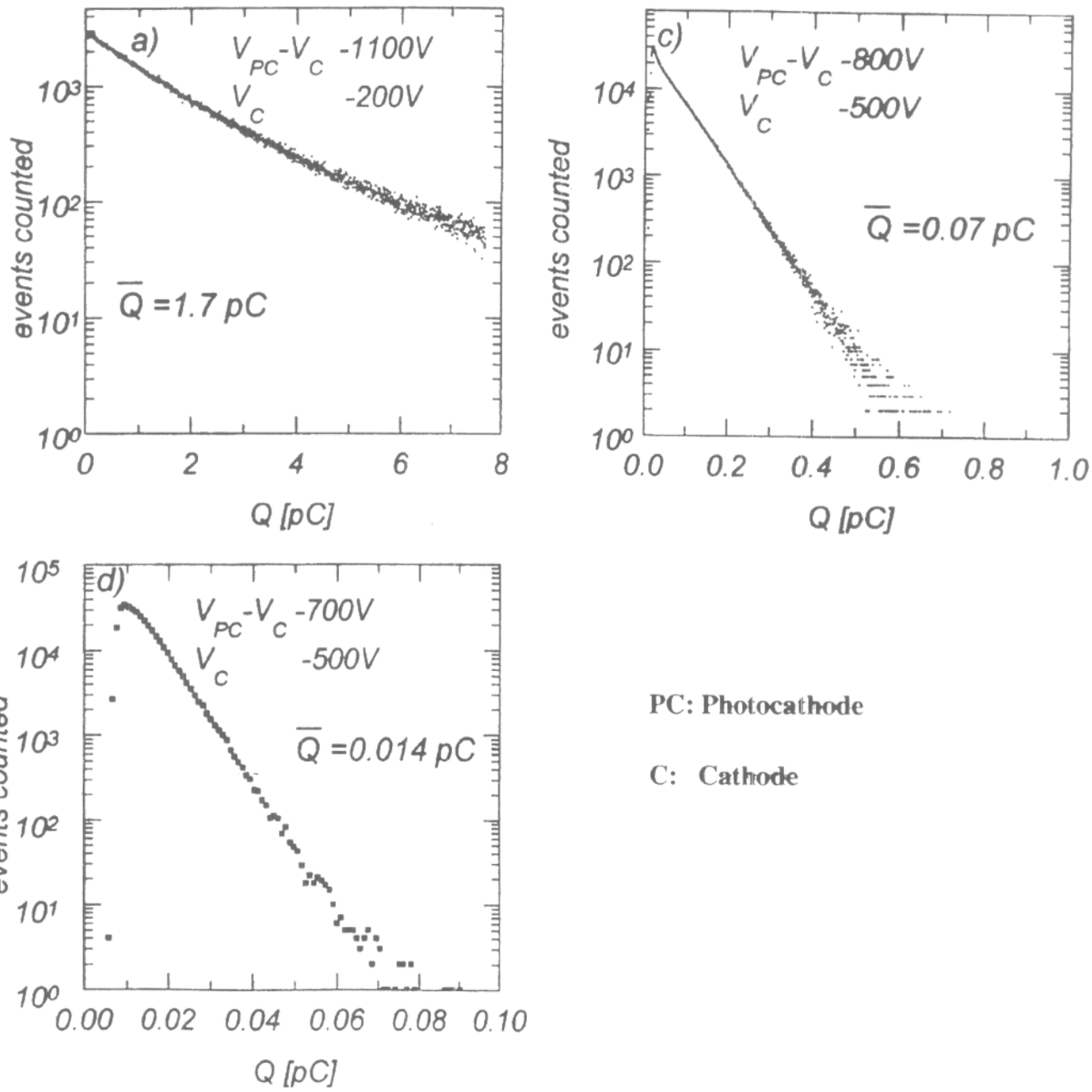

PC: Photocathode

C: Cathode

Amplification curves measured in the three operation modes for the 200 μm pitch structures

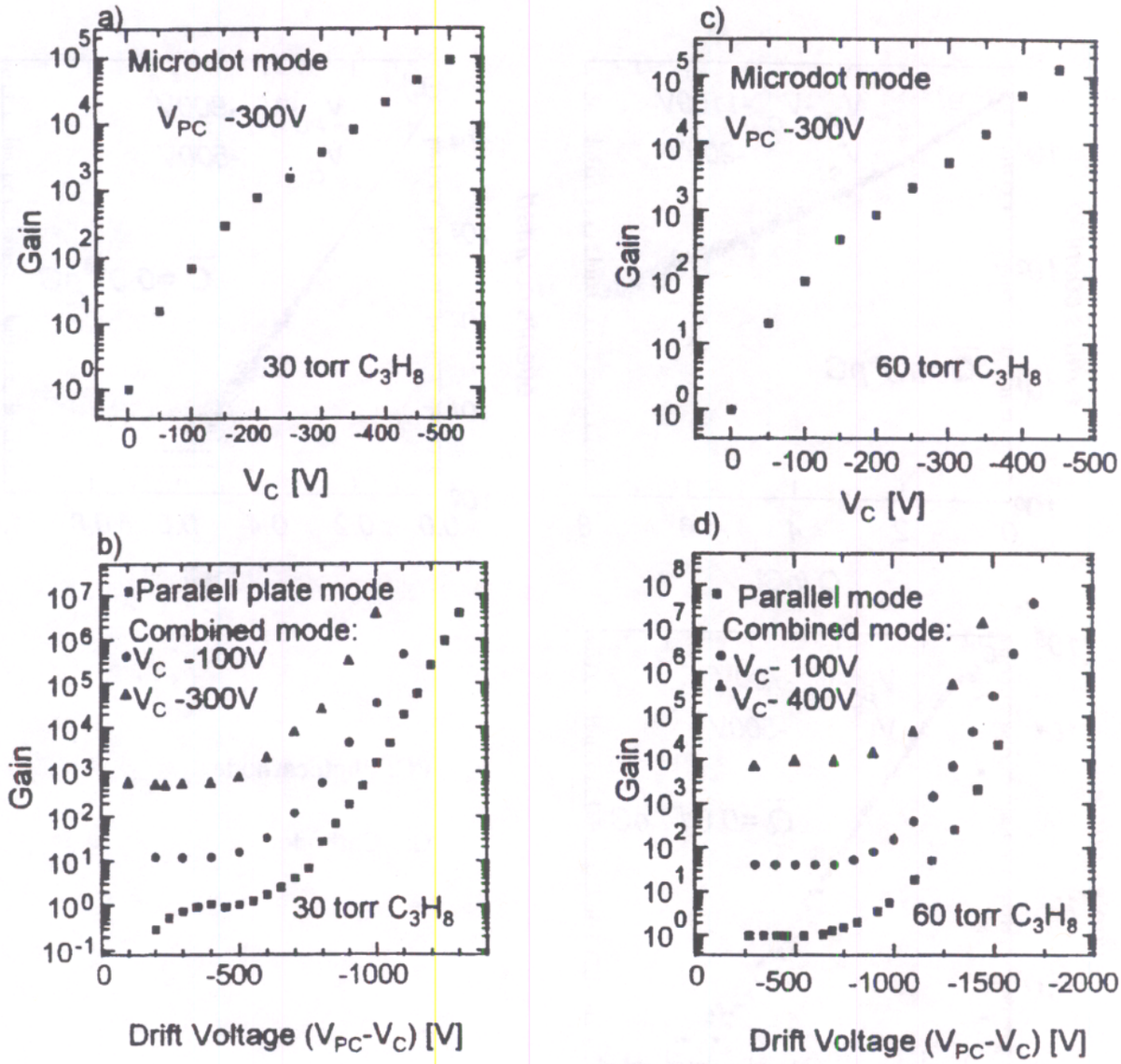

$p\rho d$ (30 torr C_3H_8, 3 mm) ≃ $p\rho d$ (20 mbar i-C_4H_{10}, 4.5 mm)

Summary and Outlook

- Solved problems: Comprehensive modeling:
  - 2D- and 3D-field strength distributions (MAXWELL)
  - LP, 2-stage avalanche multiplication, signal induction (MSGCSIM)
  - signal propagation, delay line readout (SPICE)

- Basically solved problems (production and test phase):
  - large-area, multilayer MSGC manufacturing technology:
    - two layers of metal strips (Ti/Au/Ti, Ti/Au)
    - MΩ resistive strips (Ge, Cr/SiO_2-Cermet)
    - SiO_2/DLC -doublelayer

- Presently studied or open problems:
  - linear RF magnetron sputter source with <15 g ^{157}Gd-target
  - porous SEE (e.g. CsI)
  - suppression of photon feedback: LP-GEM
  - large-area, LP MDOTs on glass substrates + array readout